AN NUMERICAL STUDY ON STEEL FIBER EFFECTS IN HIGH-STRENGTH CONCRETE SLABS

Ahmed Abdel-Aziz[1], Mahmoud Elfarnsawy[2]
, Mohamed Salah[3], Wael Ibrahim[4]

[1,3] *Civil Engineering Department, Higher Technological Institute 6 of October city, 3rd Zone, 7th section, Giza Governorate 12596, Egypt*
[2,4] *Civil Engineering Department, Faculty of Engineering at Mataria, Helwan University, Cairo 11718, Egypt*

ABSTRACT

This study explores the impact of incorporating different steel fiber volume ratios on the performance of high-strength concrete slabs. By enhancing the mechanical properties and load-carrying capacity and resistance of the concrete, steel fibers present an opportunity to reduce the reliance on traditional reinforcement bars. This approach aims to improve slab performance while potentially lowering construction costs, offering a more economical solution for structural applications

This research involved modeling and analyzing fifteen high-strength concrete slab specimens using the finite element software ABAQUS. Based on their thickness, we categorized the slabs into three groups: 8 cm, 12 cm, and 16 cm. To study the impact of thickness on the material's overall behavior. A single high-strength concrete mix design was utilized, enhanced with varying steel fiber volumetric contents: 0, 37.5, 75, and 150 kg/m³.

Additionally, to comprehensively investigate the mechanical behavior and performance characteristics of the concrete, 24 cylindrical specimens were cast for the purpose of determining the splitting tensile strength and generating the stress-strain relationship curves. Furthermore, the compressive strength of the concrete was assessed by testing 16 cast cubes, ensuring a robust evaluation of its mechanical performance

According to the results of the research, adding steel fibers to high-strength concrete slabs has a negligible effect on their compressive strength and density. Consequently, the incorporation of steel fibers into high-strength concrete slabs improves their splitting tensile strength and modulus of rupture, which in turn improves their resistance to cracking under tensile stress. This improvement is particularly relevant for structures exposed to dynamic or cyclical loading, where the risk of cracking and failure is elevated.

Keywords: - *Slabs, High-strength concrete, Compressive strength, Steel fiber, Finite Element software, Splitting tensile strength, ABAQUS.*

1. Introduction

Steel fiber reinforced concrete (SFRC) is a composite material characterized by the integration of randomly distributed steel fibers into conventional concrete. This incorporation enhances the material's properties, providing improved performance in various structural applications [1] Steel fiber typically has a tensile strength of more than 1000 MPa and excellent toughness[2]. Steel fibers serve as connectors that enhance load transfer between the aggregate and the cement mix, leading to a more consistent and homogeneous stress distribution throughout the concrete. This process diminishes stress concentrations at crack tips, so successfully preventing crack formation and propagation. Thus, the integration of steel fibers improves the overall strength and long-term durability of the concrete[3]. Numerous experiments conducted by many different researchers indicate that Steel Fiber Reinforced Concrete (SFRC) has

enhanced mechanical characteristics, including tensile strength, compressive strength, and flexural toughness, in comparison to concrete without any of steel fibers [4], [5], [6],[7],[8].

Several technical methodologies, such as macro-simulation, meso-simulation, and the damage-plasticity (CDP) model, can represent steel fiber-reinforced concrete (SFRC). The macro simulation considers SFRC in the whole of it. The model represents the effect of steel fiber reinforcement on concrete by modifying its constitutive relationship. By adjusting and modifying the parameters of the plastic damage constitutive model of concrete [9], to more accurately predict the mechanical behavior of steel fiber-reinforced concrete (SFRC), a constitutive model can be developed. [10],[11],[12],[13].

Meso-simulation is a method that employs finite element software to directly simulate the concrete mix, steel fibers, and other phase materials. This method evaluates the overall mechanical properties of Reinforced Concrete with steel fibers (by considering the interaction between the steel fiber elements and the concrete mix). Wang et al. [14] effectively integrate computational and experimental methods testing to more effectively illustrate the meso-development and alterations in the failure process of SFRC specimens through the use of MFPA^{2D} software to simulate the compressive strength test. Abbas et al. [15] predicted the full structural response of the tested beams using the established finite element models. Congro et al. [16] developed a numerical model for fiber splitting and employed a two-dimensional numerical framework to conduct the direct tensile test of steel fiber reinforced concrete SFRC. The test verification has confirmed that the suggested model accurately represents the exact behavior observed during the tensile test. Thus, computational modeling could explain the effect mechanism of steel fibers on concrete and macro-mechanical properties.

For concrete, a continuum damage model based on plasticity was used to model the damage-plasticity [17]. A scalar (isotropic) damage parameter is applied to characterize the damage model, which is integrated with elastic-plastic behavior under compressive and tensile stresses to illustrate inelastic behavior. [18]. In the finite element program ABAQUS, a model known as the concrete damage plasticity (CDP) model is incorporated to model the mechanical behavior of normal strength concrete (NSC), making it an effective tool for predicting the mechanical behavior of normal strength concrete (NSC). [19],[20],[21]. Due to the superior tensile strength and ductility of high-strength fiber-reinforced concrete (HSFRC) compared to reinforced concrete without steel fibers, the shape of the material's constitutive curve differs significantly from that of NSC in terms of its attributes. For the purpose of simulating HSFRC, it is important to calculate the parameters of the CDP model before utilizing it. The purpose of this simulation is to determine how high-strength fiber-reinforced concrete composites behave when subjected to biaxial tension. Tysmans et al. [22] implemented a CDP model. The report found that the model accurately simulated the strain hardening behavior of fiber concrete, albeit with reduced rigidity. It is important to note that the previously mentioned investigations exclusively focus on small-scale specimens without internal reinforcement, and they exclusively develop 2D finite element models. Mahmud et al.[23] and Singh et al.[24] used the UHPFRC material test to calibrate the CDP model. They then employed the calibrated model to simulate the test results of UHPFRC beam [25]. Reports indicate that the calibrated CDP model accurately and effectively estimates the plastic damage distributions and load-displacement curves of UHPFRC components.

The integration of macro-simulation, meso-simulation, and the damage-plasticity (CDP) model offers a comprehensive approach to modeling the behavior of steel fiber reinforced concrete (SFRC). Macro-simulation simplifies the representation of SFRC by adjusting the constitutive relationship of concrete to account for the influence of steel fibers, enabling the prediction of global mechanical behavior efficiently. Meso-simulation, on the other hand, provides a detailed analysis by modeling individual components of SFRC, such as the concrete matrix and steel fibers, and their interactions, allowing for a nuanced understanding of localized phenomena. When combined with the CDP model, which captures the inelastic behavior of concrete through calibrated parameters representing damage and plasticity, this approach bridges the gap between global and local analyses. The CDP model can be tailored to include the enhanced tensile strength and ductility of SFRC, ensuring accurate predictions of both macro-mechanical properties and localized damage distributions. This synergy allows for a more robust and precise simulation of SFRC's behavior under complex loading conditions.

A Steel Fiber High-Strength Concrete (SFHSC) mix was evaluated with conventional materials, standard mixing procedures, and typical curing techniques. The investigation aimed to evaluate stress-strain behavior as well as compressive and tensile strength in the material. The experimental stress-strain data collected from the tests were used to calibrate the parameters of the Concrete Damaged Plasticity (CDP) model, thereby representing the material behavior accurately.

2. Experimental Details.

2.1 Materials

2.1.1 Aggregate

For the high-strength concrete used in the study, crushed stone (dolomite) with a maximum diameter of 1 cm was used as the coarse aggregate. Natural sand (fine aggregate) was used. Sand aggregate specific gravity was 2.53, while dolomite aggregate specific gravity was 2.7.

2.1.2 Cementitious Materials

Concrete mixtures were prepared using Ordinary Portland Cement with CEM I 42.5N as the cementitious material. This type of cement meets the specifications of E.S.S.4756-1:2013 and E.S.197-1:2011[42][43], and was manufactured by the Tourah Cement Company in Egypt. In addition to OPC, micro-silica (silica fume) was added to enhance the strength of the concrete mixtures. According to ASTM C 1240 [44] the silica fume used in the study has the following characteristics: it looks like a gray powder, has a particle size of 0.2µm, a surface area of 14 m^2/g, and density of 20 kN/m^3.

2.1.3 Super-Plasticizer

Addicrete BVF was used as a super-plasticizer in the high-strength concrete mixtures, which complies with ASTM C494 Type (F) [45] and BS 5075 Part 3 [46]. The Addicrete BVF was a brown liquid with a density of 11.8 KN/m3, zero chloride content, and approximately zero air entrainment. It is compatible with all types of Portland cement and is designed to improve the workability of concrete mixtures without reducing their strength.

2.1.4 Steel fiber

The corrugated steel fibers used are shown in Fig. 1. They have a unique shape that allows them to be oriented in multiple directions, which can help to distribute stresses and strains more uniformly throughout the concrete mixture. Also, this can help to improve the load-bearing capacity. Their tensile strength is 1200 MPa, higher than conventional steel fibers.

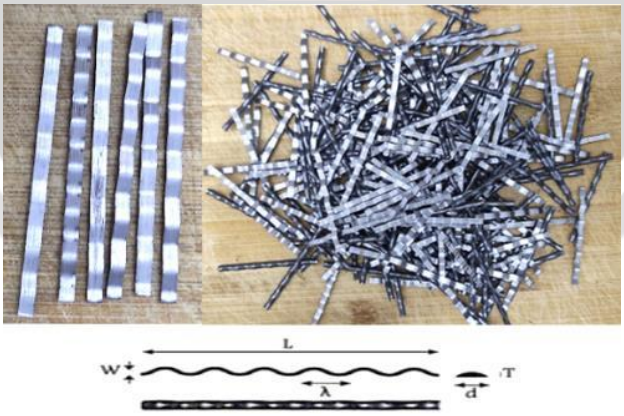

Fig. 1 : corrugated steel fibers.

The corrugated steel fibers also have a relatively low density of 7.870 Kg/m3, length (L) =50 mm ± 3 mm, width (d) = 2 mm ± 1 mm, thickness (t) = 0.7 mm ± 0.1 mm, wave depth (W)=2.0 mm ± 0.2 mm, wavelength (λ) =6.5 mm ± 0.5 mm., which can help to reduce the overall weight of the concrete slabs. This can be particularly important for large-scale concrete structures, where weight reduction can help to reduce the overall cost and complexity of the construction process.

2.2 Mix design.

ACI 211.1-91 [47] was followed in the design of four trail mixes to provide a 60 Mpa compressive strength for high-strength concrete slabs reinforced with conventional steel bars and steel fibers. Three volumetric contents of steel fibers 37.5, 75, and 150 Kg/m^3 were used in the other mixtures; the first was a control

mix without steel fiber Table 1 contains the material quantities for the water cementitious ratios and concrete mixes. Moreover 1.5 percent of the volume of steel fiber Vf lowers the workability [48].

Table 1 Quantities of materials for concrete mixtures.

Mixture ID			**M0**	**M1**	**M2**	**M3**
W/C			0.29	0.29	0.29	0.29
Concrete Ingredients (Kg/m3)	**Cement**		470	470	470	470
	Water		160	160	160	160
	Aggregate	**Dolomite**	1130	1120	1105	1080
		Sand	600	600	600	600
	Silica fume		70.5	70.5	70.5	70.5
	Super-Plasticizer		14.1	14.1	14.1	14.1
	Steel Fiber		-	37.5	75	150

2.3 The process of preparing, casting, and curing test cubes and cylinders.

As shown in Fig. 2 for each concrete mixture, four standard cubes (150x150x150) mm were cast to measure the compressive strength at 28 days. A standard cylinder (150mm in diameter, 300mm high) was cast to determine splitting tensile strength for each concrete mixture and draw stress strain curve.

Fig. 2: Standard cubes and cylinders after casting.

3. Finite Element Modeling

Fifteen slab specimens were constructed to examine the flexural properties of steel fiber high-strength concrete (SFHSC). Each slab was 500 mm in width and 1300 mm in length, with five slabs per group exhibiting varying thicknesses of 80 mm, 120 mm, and 160 mm, as illustrated in Fig. 3 The primary characteristics evaluated were the quantity of steel fibers and the rebar ratio, as indicated in Table 6.

3.1 Element Description

To develop the finite element model, a three-dimensional finite element (FE) mesh was generated for the concrete slabs and reinforcement bars, utilizing two distinct element types: the solid element for concrete slab and the truss (or wire) element for reinforcement bars.
Concrete slabs were modeled using (C3D8R) as shown in Fig. 4

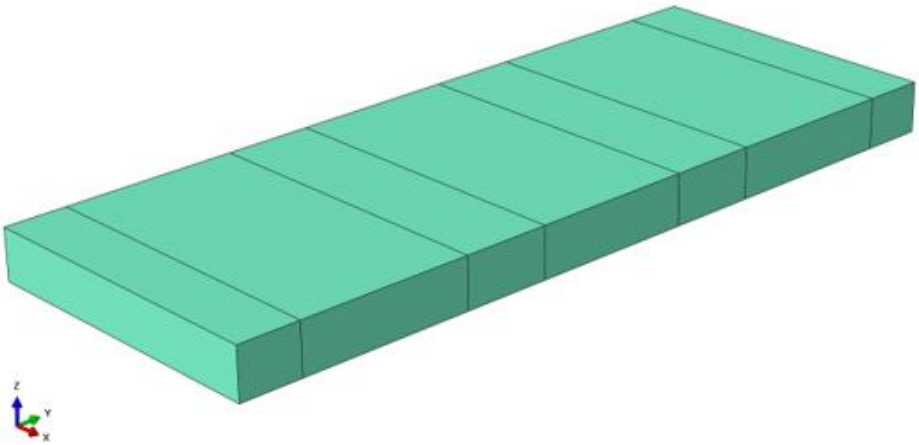

Fig. 3 Concrete slab part

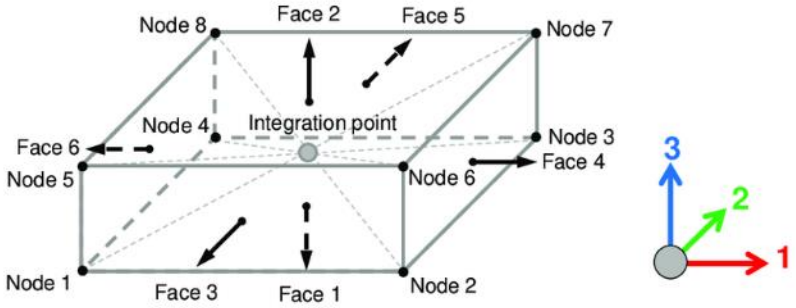

Fig. 4 Dimensional solid element

A truss element (T3D2) is a rod that can only support tensile or compressive force. It has no bending resistance. Steel reinforcement was represented using truss elements with diameters of 10 mm and 12 mm as depicted in Fig. 5

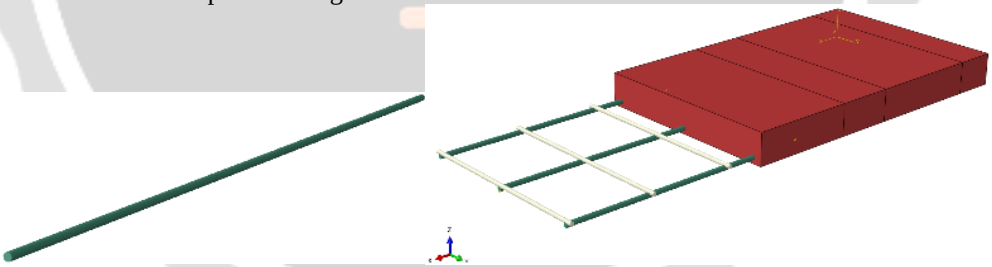

Fig. 5 Modeling of reinforcement bars

3.2 Material Modeling

All material properties for the modeled elements were specified, though high-quality data proved challenging to acquire, particularly for complex material models such as those involving damage parameters. Consequently, the accuracy of the simulation results is limited by the precision and comprehensiveness of the material data. In the modeling of reinforced concrete (RC) slabs, two distinct material models were applied: ABAQUS's concrete-damaged plasticity model was used for the concrete, while an elastic-plastic model represented the reinforcing steel embedded within the concrete matrix. Table 2 and

Table **3** show outlines of the elastic properties and concrete-damaged plasticity parameters for concrete, respectively, and

Table **4** show the details of the elastic properties of steel reinforcement.

Table 2 Elastic properties of concrete

Parameter	M0	M1	M2	M3
Density (Kg/m^3)	2925	2946	3008	3045
Modulus of elasticity (E_c)	39516.8	40192	41209.9	41781.5
Poisson's ratio	0.22	0.22	0.21	0.21

Table 3 Concrete damaged plasticity parameters

Parameter	Dilation angle	Eccentricity	fbo/fco	K	Viscosity (P)
M0	41	0.12	1.35	0.67	1.0E-05
M1	41	0.12	1.35	0.67	1.0E-05
M2	43	0.11	1.35	0.68	1.0E-05
M3	43	0.11	1.35	0.68	1.0E-05

Table 4 Elastic properties of steel reinforcement

Parameter	Mass density (MPa)	Modulus of elasticity (Es), (MPa)	Poisson's ratio
Steel Reinforcement	7.86E-09	210000	0.3

3.3 Define loads in Abaqus

For the fifteen models, the load type was specified as pressure, applied to two separate regions as shown in Fig. 6

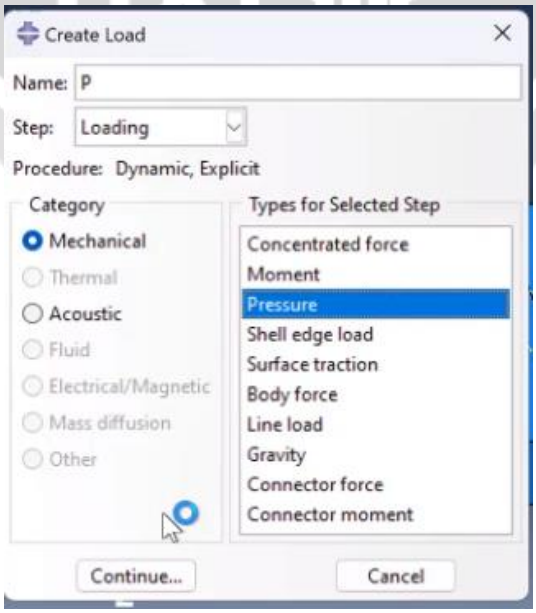

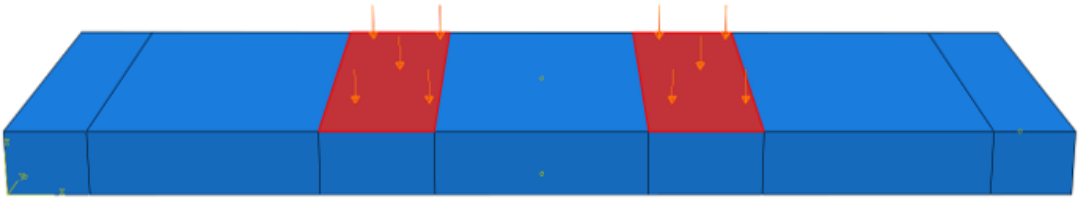

Fig. 6 Loads in the Abaqus environment

4. Results and discussion

4.1 Results of compressive strength

Compressive strength (Fcu) results of all the concrete mixtures tested after 28 days are shown in Table **5**. The Mo mixture without steel fibers achieved a compressive strength of 80.6 Mpa while the M1 mixture with steel fibers 37.5 kg/m3 reached 83.44 MPa, exceeding the control mixture (Mo) by 3.5%. The M2 mixture with 75 kg/m3 steel fibers increased to 87.72 MPa, representing an 8.74% increase over the Mo mixture. The M3 mixture with 150 kg/m3 steel fibers increased to 90.17 MPa, representing an 11.79% increase compared to the control mixture.

According to the results of the tests, the incorporation of steel fibers into HSC has the potential to slightly enhance its compressive strength. This is because the fibers serve as internal reinforcement, which reduces the formation of microcracks and prevents their spread, thereby increasing the material's load-bearing capacity. Furthermore, the very low volume fractions of steel fibers that were used in this study (up to 150 kg/m^3) are not sufficient to appreciably affect the dense microstructure of the concrete, which is the primary factor that determines compressive strength.

4.2 Results of Splitting tensile strength.

The splitting tensile strength of all the concrete mixtures tested is illustrated in Table **5** and Fig. 7. After 28 days, the Mo mixture without steel fibers achieved a splitting tensile strength of 4.83 MPa, while the M1 mixture with steel fibers 37.5 kg/m3 increases to 9.11 MPa, representing an 88.5 % increase over Mo mixture without steel fibers. The M2 mixture with 75 kg/m3 steel fibers had a strength of 10.67 Mpa which is a 120.7% increase compared to the Mo mixture. Finally, the M3 mixture with 150 kg/m3 steel fibers had a strength of 13.14 MPa, which is a 171.9% increase compared to the Mo mixture.

Table 5: Compressive strength and splitting tensile strength results

Mixture Id	Steel Fiber (Kg/m3)	Compressive strength results			Splitting tensile strength results	
		Density (Kg/m3)	Failure Load (KN)	Compressive Strength (Mpa)	Failure Load (KN)	Splitting tensile strength (Mpa)
Mo	-	2925.5	1814.96	80.66	217.5	4.83
M1	37.5	2947	1877.43	83.44	410	9.11
M2	75	3008.3	1973.72	87.72	480	10.66
M3	150	3045.1	2028.94	90.17	591.5	13.14

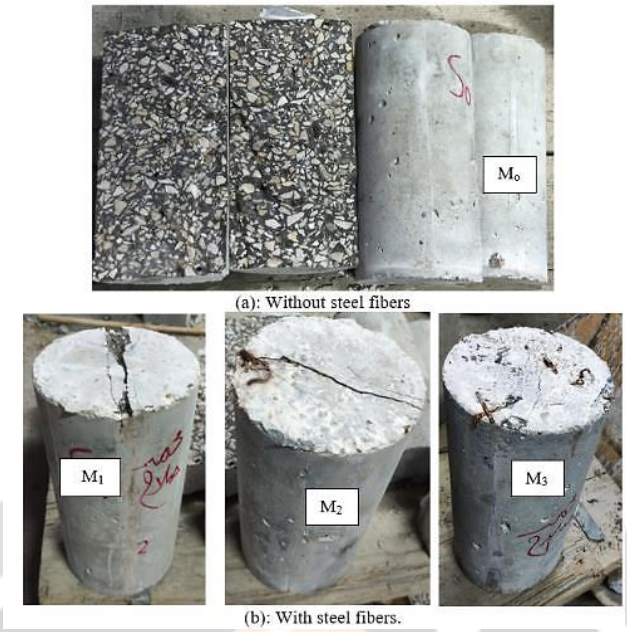

Fig. 7 Splitting tensile failure for cylinders.

Incorporating fibers into concrete can greatly improve its splitting tensile strength. This improvement is due to the fiber's ability to prevent or delay the propagation of cracks, which is achieved through the fiber's high tensile strength and toughness. When a crack forms in concrete, the fiber prevents the crack from expanding as shown in Fig. 7. By preventing the growth of cracks, fibers can help maintain the concrete's load-bearing capacity, even under tensile stress.

4.3 Stress strain curve

One important feature of the performance of steel fiber-reinforced concrete (SFRC) is its stress-strain behavior, which demonstrates the material's mechanical response under loading. Fig. 8 presents stress-strain curves for various concrete mixtures with different steel fiber content. The results indicate that increasing the steel fiber content significantly enhances the concrete's ductility and toughness. Mixtures with 150 kg/m³ of steel fibers exhibited a higher peak stress and sustained strain beyond the elastic range, demonstrating superior energy absorption compared to control mixtures. This improvement is attributed to the fibers' ability to bridge microcracks and distribute stresses more evenly, thereby delaying crack propagation and enhancing the composite material's overall load-bearing capacity.

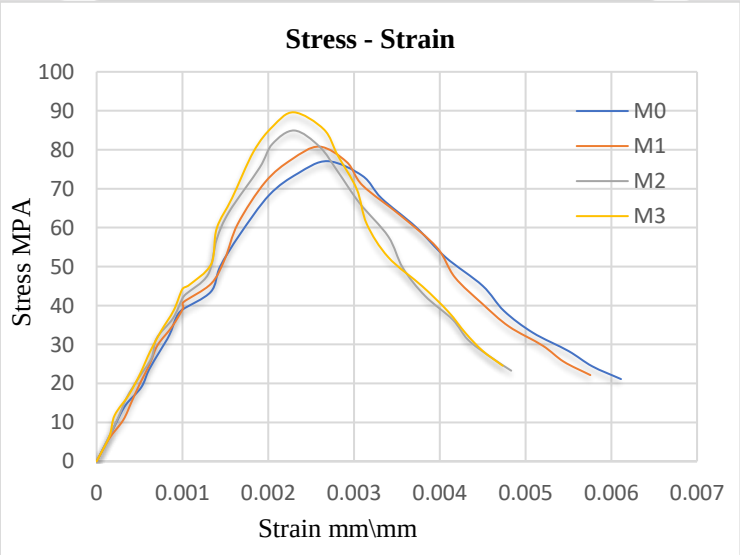

Fig. 8 Stress-Strain Curves

4.4 Cracks pattern and failure modes

Based on the tension damage contour plots, the failure pattern observed in the FEM analyses of slabs reinforced with steel bars displayed a ductile failure mode. The numerically derived crack patterns are illustrated in the following figures.

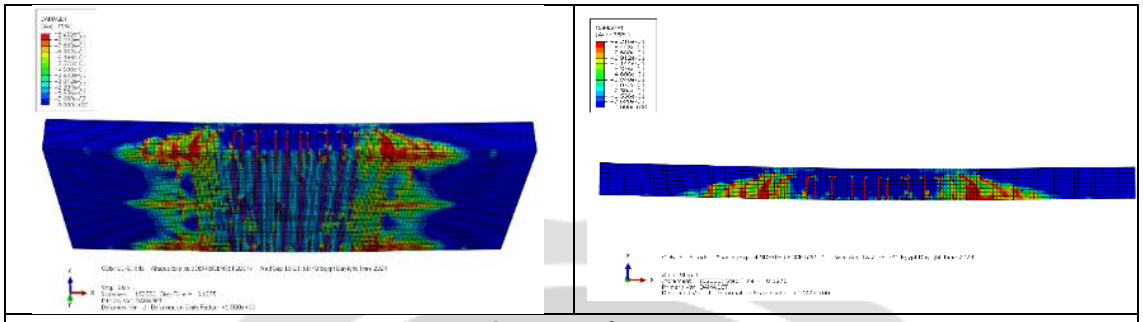

Cracks pattern for S0-80

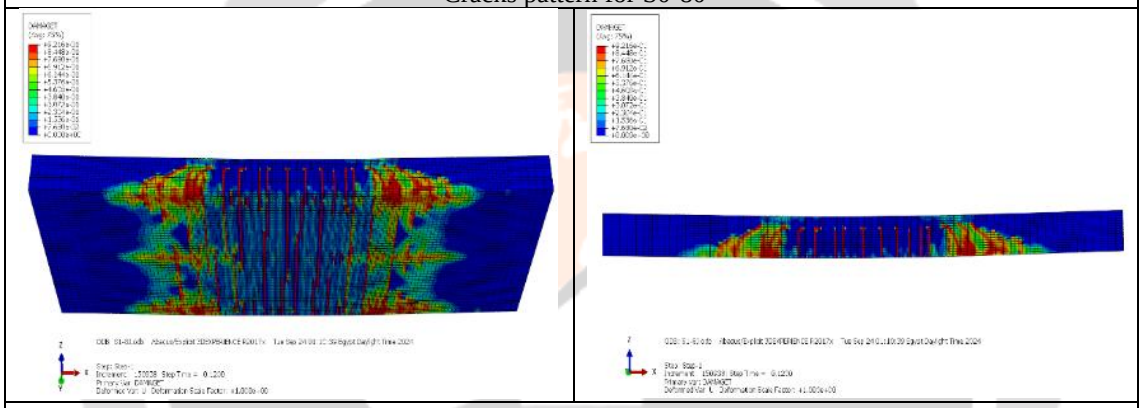

Cracks pattern for S1-80

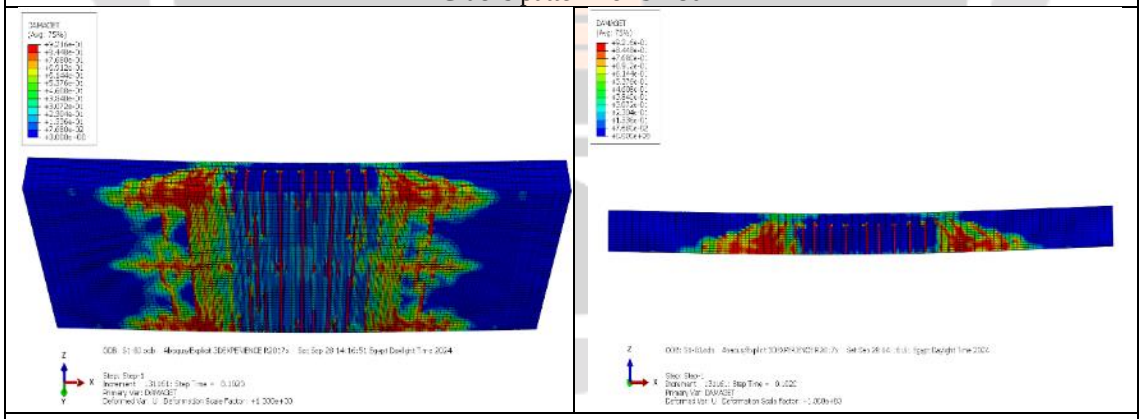

Cracks pattern for S2-80

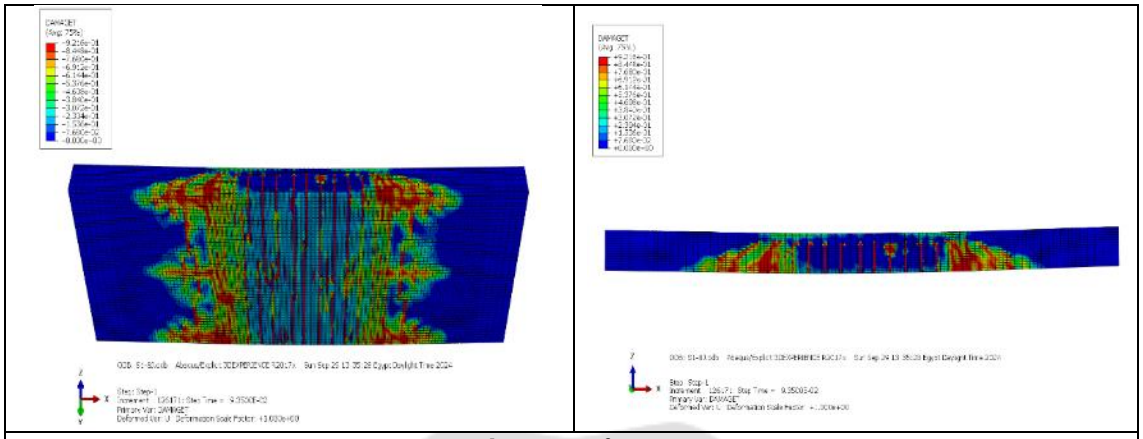

Cracks pattern for S3-80

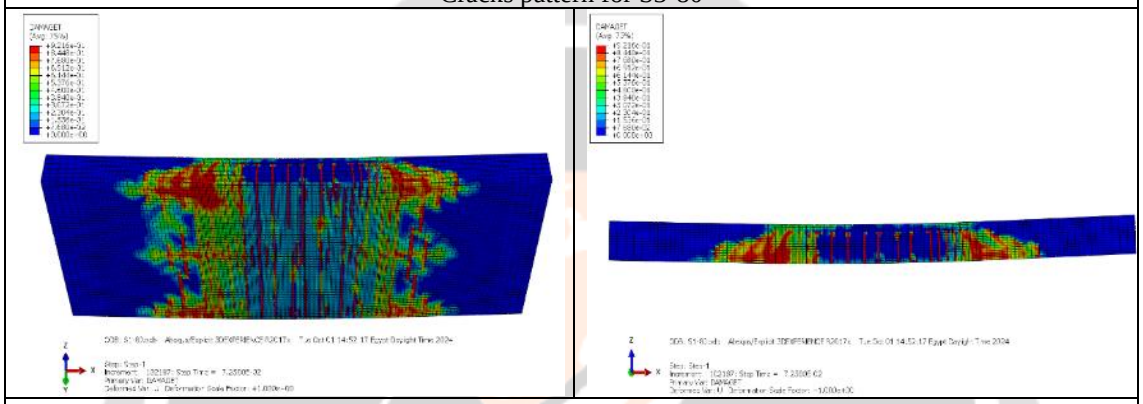

Cracks pattern for S4-80

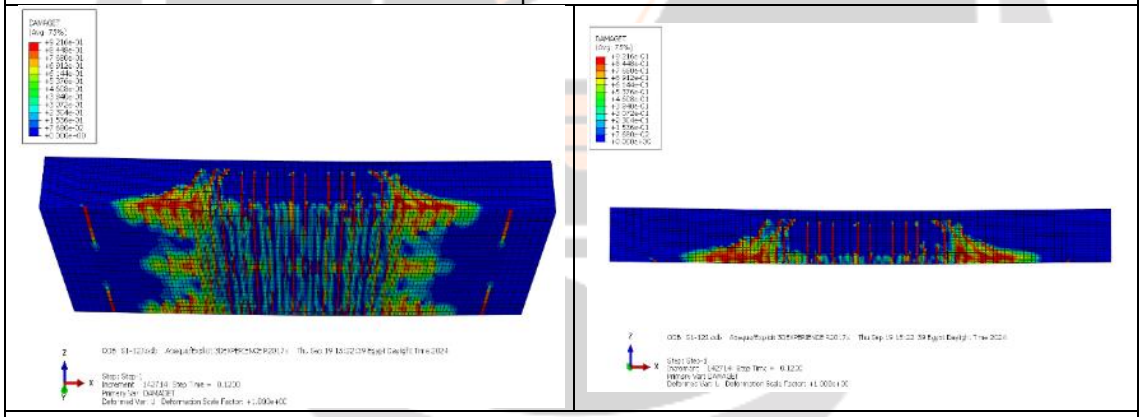

Cracks pattern for S0-120

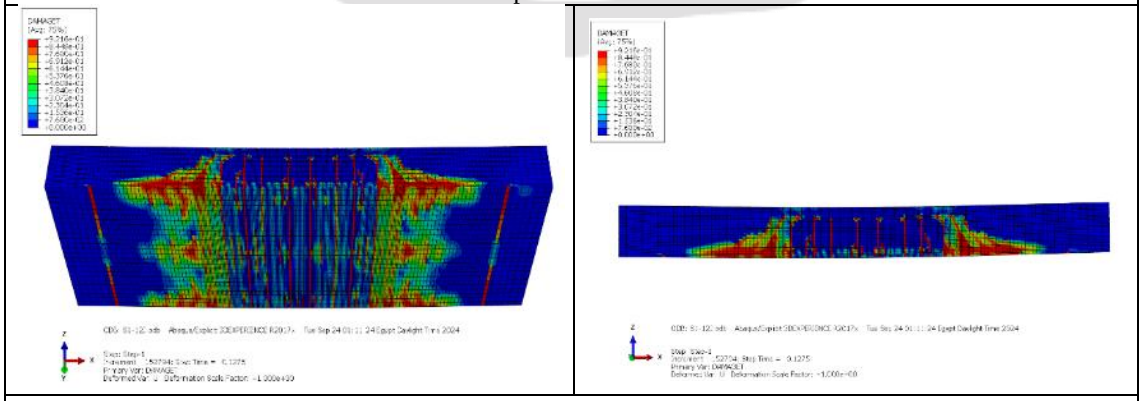

Cracks pattern for S1-120

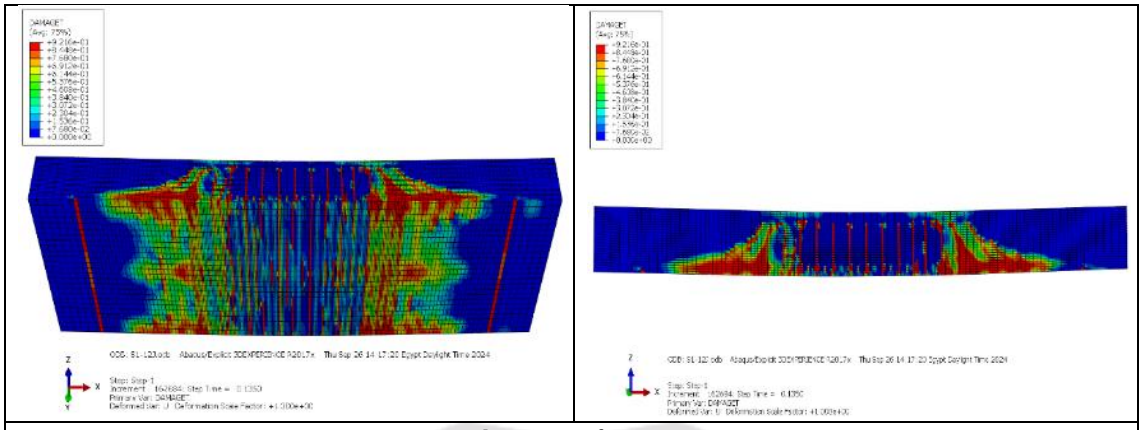

Cracks pattern for S2-120

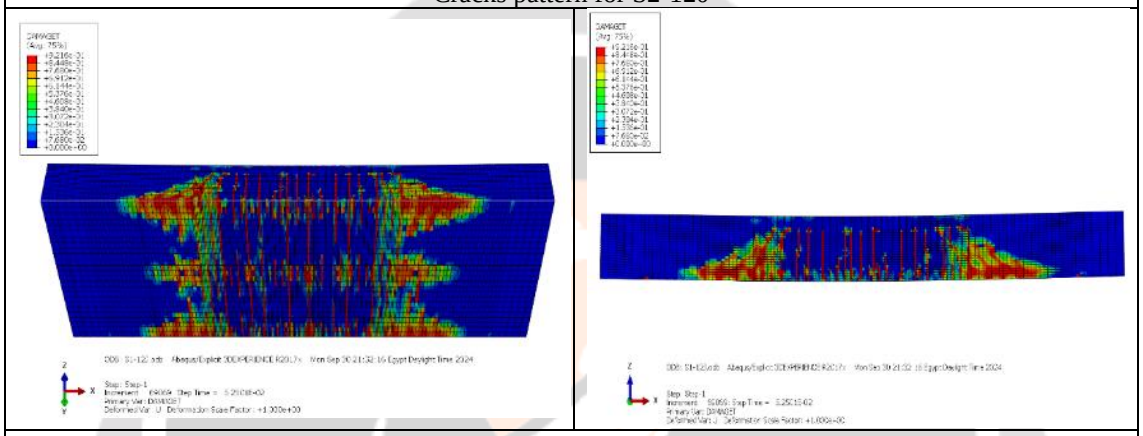

Cracks pattern for S3-120

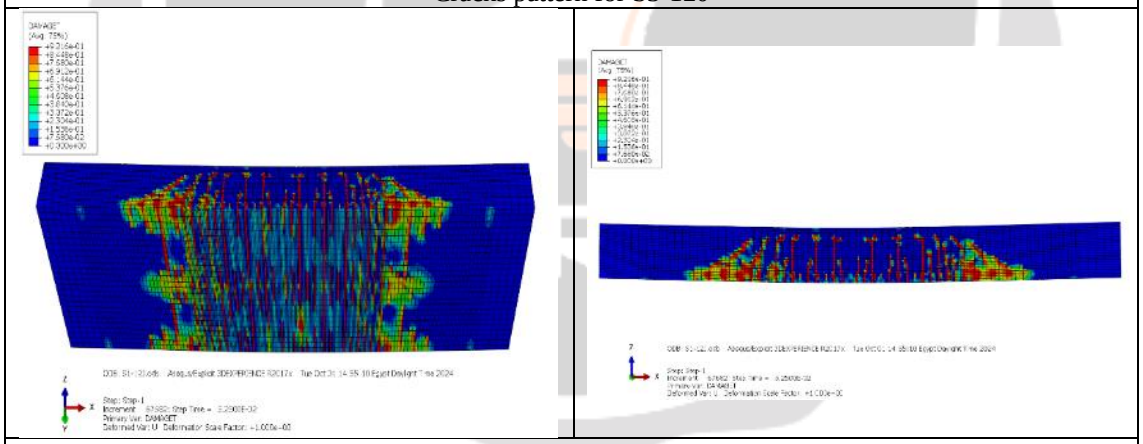

Cracks pattern for S4-120

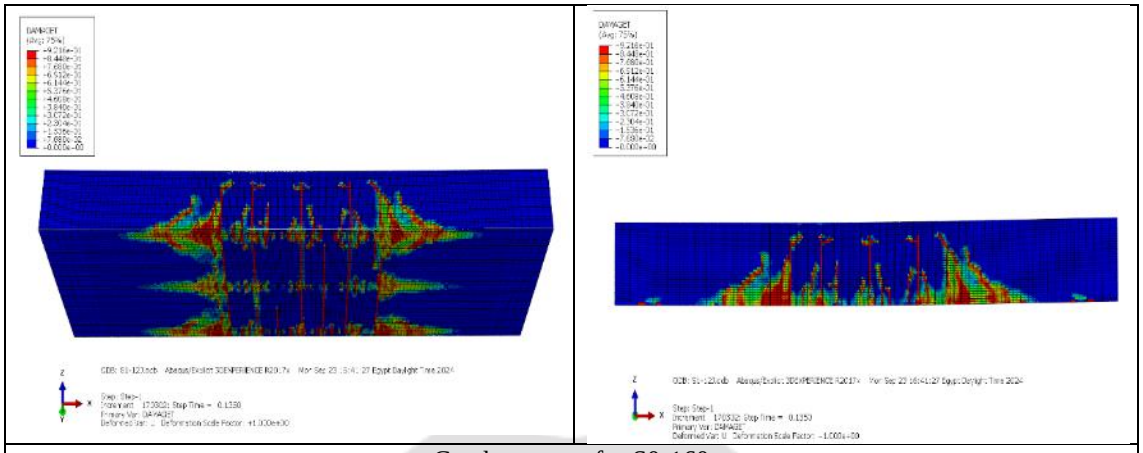

Cracks pattern for S0-160

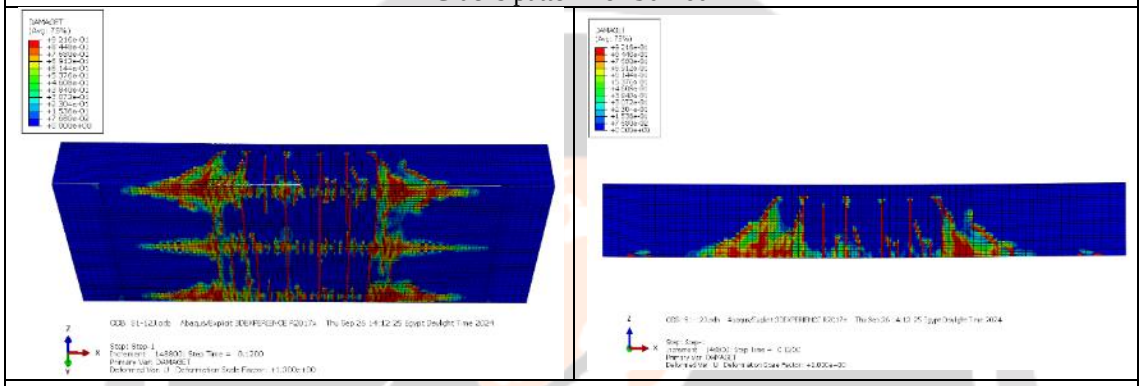

Cracks pattern for S1-160

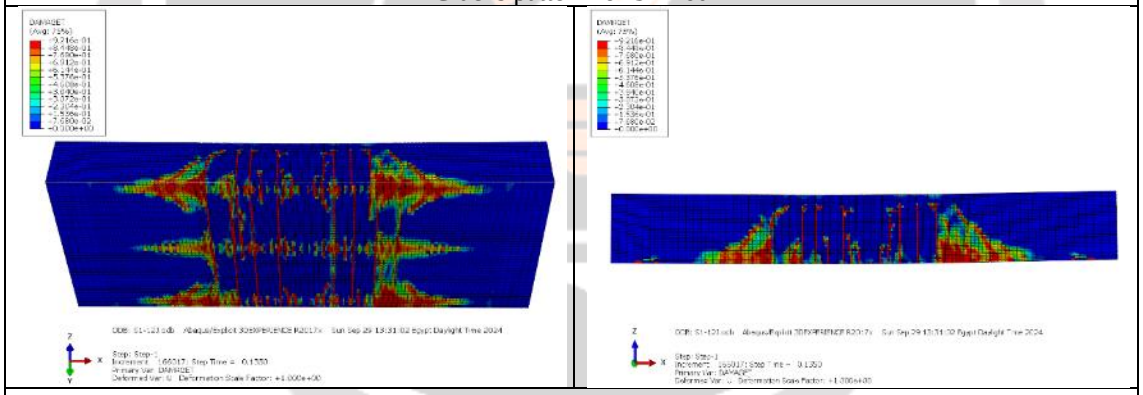

Cracks pattern for S2-160

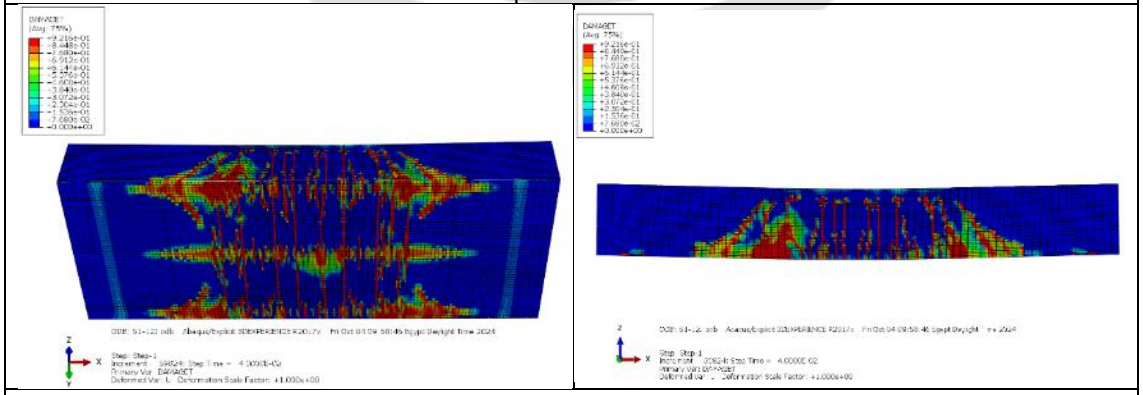

Cracks pattern for S3-160

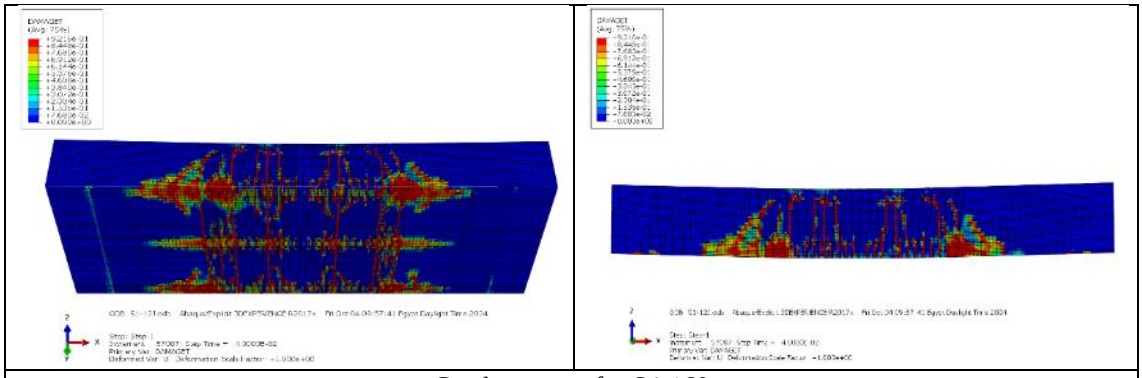

Cracks pattern for S4-160

Fig. 9 Cracks pattern for slabs

The results from the numerical analysis clearly demonstrate that incorporating steel fibers significantly influences the crack patterns and failure modes of high-strength concrete slabs. The tension damage contour plots reveal a shift from brittle to more ductile failure modes as the steel fiber content increases. This improvement is attributed to the fibers' ability to arrest crack propagation and distribute stress more evenly. The addition of steel fibers not only mitigates the extent of cracking but also enhances the structural resilience of the slabs under applied loads. These findings underline the efficacy of steel fiber reinforcement in improving the durability and performance of high-strength concrete, particularly in applications subjected to tensile stresses

4.5 Load-deflection results.

Table 6 and Fig. 11 illustrate the load-deflection relationship at mid-span for concrete slabs in three groups, without and with steel fibers. Adding steel fibers increased the failure load and decreased the vertical deflection at the failure load for all slabs in all groups. For group 1, the control slab (S0-80) without steel fibers had a failure load of 65.32 KN and vertical deflection of 20.0 mm. Adding steel fibers at 37.5 kg/m3 and the same reinforcement ratio for (S1-80) increased the failure load to 71.89 KN (10.0% increase over S0) and vertical deflection to 20.83 mm. Adding steel fibers at 75 kg/m3 for (S2-80) with the same reinforcement ratio increased the failure load to 74.02 KN (13.3 % increase over S0) and decreased the vertical deflection to 18.06 mm. For the same reinforcement ratio while increasing the steel fiber ratio to 150 kg/m3 for (S3-80) the failure load increased to 75.30 KN (15.3 % increase from S0) and decreased the vertical deflection to 17.90 mm. Otherwise for a smaller reinforcement ratio (S4-80) with the same steel fibers at 150 kg/m3, the failure load increased to 67.12 KN (2.8 % increase over S0) and decreased the vertical deflection to 16.44 mm.

For group 2, the control slab (S0-120) without steel fibers had a failure load of 119.95 KN and vertical deflection of 16.15 mm. Adding steel fibers at 37.5 kg/m3 and the same reinforcement ratio for (S1-120) increased the failure load to 128.45 KN (7.1 % increase over S0) and vertical deflection to 16.61 mm. Adding steel fibers at 75 kg/m3 for (S2-120) with the same reinforcement ratio increased the failure load to 131.79KN (9.9 % increase over S0) and decreased the vertical deflection to 16.10 mm. For the same reinforcement ratio while increasing the steel fiber ratio to 150 kg/m3 for (S3-120) the failure load increased to 139.04 KN (15.9 % increase from S0) and decreased the vertical deflection to 11.66 mm. Otherwise for a smaller reinforcement ratio (S4-120) with the same steel fibers at 150 kg/m3, the failure load increased to 120.04 KN (0.1 % increase over S0) and decreased the vertical deflection to 12.56 mm.

In group 3; the load failure for the control slab (S0-160) without steel fibers was 162.22 KN and vertical deflection was 12.03 mm. The failure load and vertical deflection have increased for (S1-160) to 174.56 KN and 12.69 mm respectively. Otherwise, the failure load for (S2-160) has increased to 181.22 KN (11.7 % increase from S0) and the vertical deflection has decreased to 9.97 mm. For (S3-160), the failure load has increased to 194.25 KN (19.7 % increase from S0), and the vertical deflection has decreased to 9.0 mm. For the last specimen (S4-160) with steel fibers 150 kg/m3 and a smaller reinforcement ratio than other specimens, the failure load increased to 177.55 KN (9.4 % increase over S0) and decreased the vertical deflection to 9.60 mm.

Table 6: Structural slab details and Load deflection

Slab Dimensions	Slab Code	Steel fiber	Pu KN	Δu mm	As main\m		As Secondary\m	
		Kg/m^3			N	Φ (mm)	N	Φ (mm)
Group (1) B=0.5m L=1.3m ts=0.08m	S0-80	-	65.32	20.00	5	12	4	10
	S1-80	37.5	71.89	20.83				
	S2-80	75	74.02	18.06				
	S3-80	150	75.30	17.90				
	S4-80	150	67.12	16.44	5	10		
Group (2) B=0.5m L=1.3m ts=0.12m	S0-120	-	119.95	16.15	5	12	4	10
	S1-120	37.5	128.45	16.61				
	S2-120	75	131.79	16.10				
	S3-120	150	139.04	11.66				
	S4-120	150	120.04	12.56	5	10		
Group (3) B=0.5m L=1.3m ts=0.16m	S0-160	-	162.22	12.03	5	12	4	10
	S1-160	37.5	174.56	12.69				
	S2-160	75	181.22	9.97				
	S3-160	150	194.25	9.00				
	S4-160	150	177.55	9.60	5	10		

Where: B: Width of slab -L: Length of slab -ts: Thickness of slab -As: Reinforcement- N: Number of bars- Φ: Bar diameter (mm)- Pu: Failure Load, -Δu: Deflection at failure load

The test results show that steel fibers can greatly increase the load-bearing capacity of concrete structures, as well as enhance their toughness in addition to these benefits, the use of steel fibers can also reduce the amount of conventional reinforcement required in concrete structures, leading to cost savings and a more sustainable construction process.

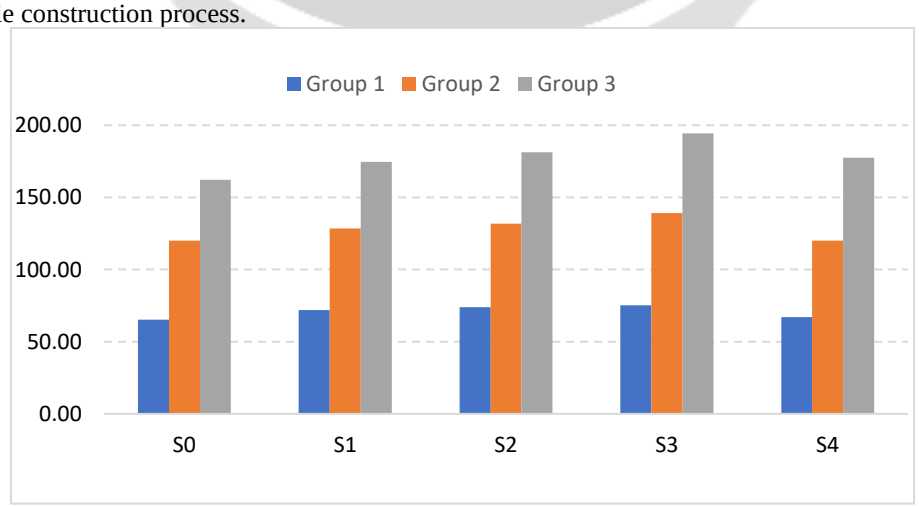

Fig. 10: Failure loads (KN) for Group 1, Group 2, and Group 3 slabs

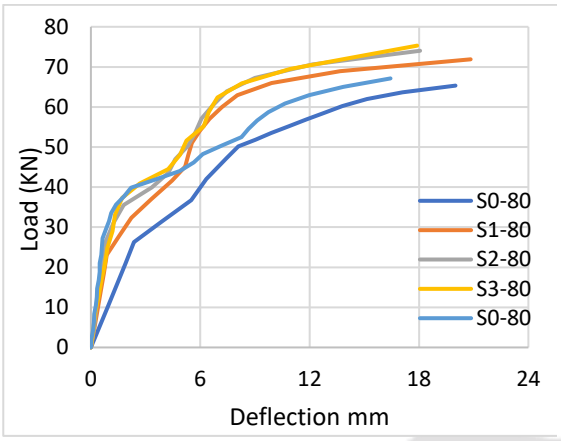

a) slabs in group 1

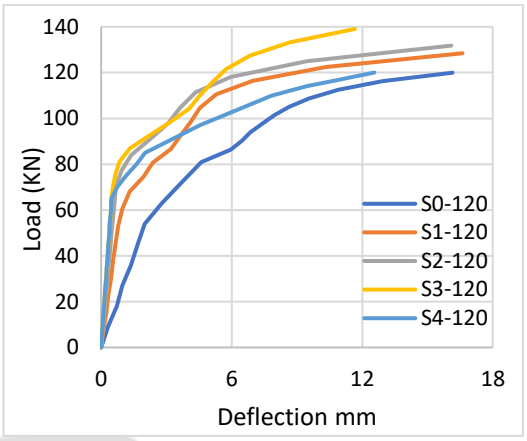

b) slabs in group 2

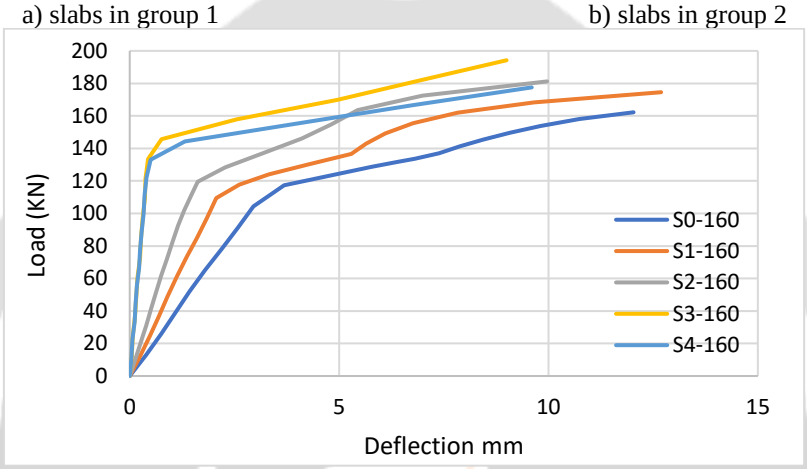

c) slabs in group 3

Fig. 11 Load deflection curves

5. Conclusions

This study evaluated the influence of adding steel fibers at varying ratios (37.5, 75, and 150 kg/m³) on the mechanical properties of high-strength concrete slabs. The results demonstrated that while the addition of steel fibers had a minimal impact on compressive strength, with a maximum increase of 11.79%, it significantly enhanced the splitting tensile strength, achieving an increase of up to 171.9%. Furthermore, steel fibers improved the modulus of rupture, reduced ultimate displacement, and increased the ductility index, making the slabs more resistant to cracking and failure under tensile stresses.

The use of the Abaqus program was instrumental in accurately representing the behavior of steel fiber-reinforced concrete (SFRC). Abaqus provided advanced simulation capabilities, such as modeling the interaction between steel fibers and the concrete matrix, which allowed for a detailed analysis of the composite material's performance. This enabled the study to capture the effects of steel fibers on crack propagation, load distribution, and the overall mechanical properties of the slabs. The software's ability to simulate nonlinear material behavior and complex load conditions was critical in validating the experimental results and gaining deeper insights into the structural benefits of SFRC.

Additionally, the study showed that steel fibers could effectively reduce the required reinforcement ratios without compromising structural integrity. For example, slabs containing 150 kg/m³ of steel fibers exhibited a 15.3% higher failure load compared to control slabs, even with reduced reinforcement. This suggests that steel fibers can serve as a cost-effective and sustainable alternative to traditional reinforcement methods, leading to material efficiency and lower construction costs. The findings underscore the potential of steel fiber-reinforced concrete as a durable and economical solution for applications requiring enhanced toughness, ductility, and resistance to loading.

6. REFERENCES

[1] R. F. Zollo, "Fiber-reinforced concrete: an overview after 30 years of development," *Cem. Concr. Compos.*, vol. 19, no. 2, pp. 107–122, 1997.

[2] V. Afroughsabet, L. Biolzi, and T. Ozbakkaloglu, "High-performance fiber-reinforced concrete: a review," *J. Mater. Sci.*, vol. 51, pp. 6517–6551, 2016.

[3] J. A. O. Barros, "Steel fibre reinforced concrete: Material properties and structural applications," in *Fibrous and composite materials for civil engineering applications*, Elsevier, 2011, pp. 95–155.

[4] S. Peng, B. Wu, X. Du, Y. Zhao, and Z. Yu, "Study on dynamic splitting tensile mechanical properties and microscopic mechanism analysis of steel fiber reinforced concrete," in *Structures*, 2023, vol. 58, p. 105502.

[5] Z. Wu, C. Shi, W. He, and L. Wu, "Effects of steel fiber content and shape on mechanical properties of ultra high performance concrete," *Constr. Build. Mater.*, vol. 103, pp. 8–14, 2016.

[6] V. Gokulnath, B. Ramesh, and S. Sivashankar, "Influence of M sand in self compacting concrete with addition of steel fiber," *Mater. Today Proc.*, vol. 22, pp. 1026–1030, 2020.

[7] A. G. Bajgirani, S. Moghadam, S. T. Tafreshi, A. Arbab, and H. Razeghi, "The Influence of Aspect Ratio of Steel Fibers on The Mechanical Properties of Concrete," *CiteSeerX*, no. July, pp. 1–8, 2016.

[8] Z. Que *et al.*, "Predicting the tensile strength of ultra-high performance concrete: New insights into the synergistic effects of steel fiber geometry and distribution," *Constr. Build. Mater.*, vol. 444, p. 137822, 2024.

[9] P. H. Feenstra and R. De Borst, "A composite plasticity model for concrete," *Int. J. Solids Struct.*, vol. 33, no. 5, pp. 707–730, 1996.

[10] J. BI, L. HUO, H. QIAO, and Y. Zhao, "A constitutive model of steel fiber reinforced concrete under uniaxial tension," *Eng. Mech.*, vol. 37, no. 6, pp. 155–164, 2020.

[11] Y. CHI, L. HUANG, and M. YU, "Calibration method of damage plasticity model for steel-polypropylene hybrid fiber reinforced concrete based on ABAQUS," *Eng. Mech.*, vol. 34, no. 12, pp. 131–142, 2017.

[12] Z. Li, Z. Peng, and J. Teng, "Study of combined multi-point constraint multi-scale modeling strategy for ultra-high-performance steel fiber-reinforced concrete structures," *Materials (Basel).*, vol. 13, no. 23, p. 5320, 2020.

[13] Y. Chi, M. Yu, L. Huang, and L. Xu, "Finite element modeling of steel-polypropylene hybrid fiber reinforced concrete using modified concrete damaged plasticity," *Eng. Struct.*, vol. 148, pp. 23–35, 2017.

[14] F. Lu, J. Xu, W. Li, Y. Hou, F. Qin, and M. Pan, "Study on multi-scale damage and failure mechanism of steel fiber reinforced concrete: Experimental and numerical analysis," in *Structures*, 2023, vol. 48, pp. 768–781.

[15] Y. M. Abbas, A. Tuken, and N. A. Siddiqui, "Improving the structural behavior of shear-deficient RC deep beams using steel fibers: Experimental, numerical and probabilistic approach," *J. Build. Eng.*, vol. 46, p. 103711, 2022.

[16] M. Congro, E. C. M. Sanchez, D. Roehl, and E. Marangon, "Fracture modeling of fiber reinforced concrete in a multiscale approach," *Compos. Part B Eng.*, vol. 174, p. 106958, 2019.

[17] J. Lubliner, J. Oliver, S. Oller, and Ejij. Onate, "A plastic-damage model for concrete," *Int. J. Solids Struct.*, vol. 25, no. 3, pp. 299–326, 1989.

[18] A. Abrishambaf, J. A. O. Barros, and V. M. C. F. Cunha, "Tensile stress–crack width law for steel fibre reinforced self-compacting concrete obtained from indirect (splitting) tensile tests," *Cem. Concr. Compos.*, vol. 57, pp. 153–165, 2015.

[19] G. M. Chen, J. F. Chen, and J. G. Teng, "On the finite element modelling of RC beams shear-strengthened with FRP," *Constr. Build. Mater.*, vol. 32, pp. 13–26, 2012.

[20] S. Q. Li, J. F. Chen, L. A. Bisby, Y. M. Hu, and J. G. Teng, "Strain efficiency of FRP jackets in FRP-confined concrete-filled circular steel tubes," *Int. J. Struct. Stab. Dyn.*, vol. 12, no. 01, pp. 75–94, 2012.

[21] J. F. Chen, G. M. Chen, and J. G. Teng, "Role of bond modelling in predicting the behaviour of RC beams shear-strengthened with FRP U-jackets, keynote," in *Proceedings of the 9th International Symposium on Fibre Reinforced Polymer for Concrete Structures (FRPRCS9)*, 2009.

[22] T. Tysmans, M. Wozniak, O. Remy, and J. Vantomme, "Finite element modelling of the biaxial behaviour of high-performance fibre-reinforced cement composites (HPFRCC) using Concrete

Damaged Plasticity," *Finite Elem. Anal. Des.*, vol. 100, pp. 47–53, 2015.
[23] G. H. Mahmud, Z. Yang, and A. M. T. Hassan, "Experimental and numerical studies of size effects of Ultra High Performance Steel Fibre Reinforced Concrete (UHPFRC) beams," *Constr. Build. Mater.*, vol. 48, pp. 1027–1034, 2013.
[24] M. Singh, A. H. Sheikh, M. S. M. Ali, P. Visintin, and M. C. Griffith, "Experimental and numerical study of the flexural behaviour of ultra-high performance fibre reinforced concrete beams," *Constr. Build. Mater.*, vol. 138, pp. 12–25, 2017.
[25] I. H. Yang, C. Joh, and B.-S. Kim, "Structural behavior of ultra high performance concrete beams subjected to bending," *Eng. Struct.*, vol. 32, no. 11, pp. 3478–3487, 2010.
[26] A. Caggiano, G. Etse, and E. Martinelli, "Zero-thickness interface model formulation for failure behavior of fiber-reinforced cementitious composites," *Comput. Struct.*, vol. 98, pp. 23–32, 2012.
[27] U. Nyström and K. Gylltoft, "Comparative numerical studies of projectile impacts on plain and steel-fibre reinforced concrete," *Int. J. Impact Eng.*, vol. 38, no. 2–3, pp. 95–105, 2011.
[28] M. J. Shannag, R. Brincker, and W. Hansen, "Pullout behavior of steel fibers from cement-based composites," *Cem. Concr. Res.*, vol. 27, no. 6, pp. 925–936, 1997.
[29] T. Soetens, A. Van Gysel, S. Matthys, and L. Taerwe, "A semi-analytical model to predict the pull-out behaviour of inclined hooked-end steel fibres," *Constr. Build. Mater.*, vol. 43, pp. 253–265, 2013.
[30] M. Tuyan and H. Yazıcı, "Pull-out behavior of single steel fiber from SIFCON matrix," *Constr. Build. Mater.*, vol. 35, pp. 571–577, 2012.
[31] Y. Shi, Z.-X. Li, and H. Hao, "Bond slip modelling and its effect on numerical analysis of blast-induced responses of RC columns," *Struct. Eng. Mech.*, vol. 32, no. 2, pp. 251–267, 2009.
[32] N. Ganesan, P. V Indira, and M. V Sabeena, "Bond stress slip response of bars embedded in hybrid fibre reinforced high performance concrete," *Constr. Build. Mater.*, vol. 50, pp. 108–115, 2014.
[33] F. Aslani and S. Nejadi, "Bond characteristics of steel fibre reinforced self-compacting concrete," *Can. J. Civ. Eng.*, vol. 39, no. 7, pp. 834–848, 2012.
[34] S. Marfia and E. Sacco, "Numerical techniques for the analysis of crack propagation in cohesive materials," *Int. J. Numer. Methods Eng.*, vol. 57, no. 11, pp. 1577–1602, 2003.
[35] J. Oliver, D. F. Mora, A. E. Huespe, and R. Weyler, "A micromorphic model for steel fiber reinforced concrete," *Int. J. Solids Struct.*, vol. 49, no. 21, pp. 2990–3007, 2012.
[36] Z. Xu, H. Hao, and H. N. Li, "Mesoscale modelling of fibre reinforced concrete material under compressive impact loading," *Constr. Build. Mater.*, vol. 26, no. 1, pp. 274–288, 2012.
[37] E. Gal and R. Kryvoruk, "Meso-scale analysis of FRC using a two-step homogenization approach," *Comput. Struct.*, vol. 89, no. 11–12, pp. 921–929, 2011.
[38] E.-H. Yang, S. Wang, Y. Yang, and V. C. Li, "Fiber-bridging constitutive law of engineered cementitious composites," *J. Adv. Concr. Technol.*, vol. 6, no. 1, pp. 181–193, 2008.
[39] E. A. Schauffert and G. Cusatis, "Lattice discrete particle model for fiber-reinforced concrete. I: Theory," *J. Eng. Mech.*, vol. 138, no. 7, pp. 826–833, 2012.
[40] Q. Fang and J. Zhang, "Three-dimensional modelling of steel fiber reinforced concrete material under intense dynamic loading," *Constr. Build. Mater.*, vol. 44, pp. 118–132, 2013.
[41] X. Liang and C. Wu, "Meso-scale modelling of steel fibre reinforced concrete with high strength," *Constr. Build. Mater.*, vol. 165, pp. 187–198, 2018.
[42] 4756-1 ESS., "Egyptian organization for standard and quality, chemical, cement (part 1), composition and specifications," 2013.
[43] B. S. EN, "197-1. Cement–Part 1: Composition, specifications and conformity criteria for common cements," *London Eur. Comm. Stand.*, 2011.
[44] M. AASHTO, "307 ASTM C 1240.'Standard Specification for Silica Fume Used in Cementitious Mixtures,'" *Am. Soc. Test. Mater. Annu. B. ASTM Stand. Vol.*, vol. 2.
[45] C494M-19 AC., "Standard Specification for Chemical Admixtures for Concrete, ASTM International, West Conshohocken, PA.," 2019.
[46] B. S. Institution, *Concrete Admixtures: Specifications for Superplasticizing Admixtures*. BSI, 1985.
[47] 211.1-91, "A. American concrete institute, Standard Practice for Selecting Proportions for Normal, Heavyweight, and Mass Concrete.".
[48] J. Katzer and J. Domski, "Quality and mechanical properties of engineered steel fibres used as reinforcement for concrete," *Constr. Build. Mater.*, vol. 34, pp. 243–248, 2012.